

Experimental Investigation of the Electro Co-deposition of (Zinc-Nickel) Alloy

Ekhlas Abdulrahman Salman

Assistant Lecture

Engineering College- Al-Nahrain University

E-mail:ysarslman@gmail.com

ABSTRACT

An experimental investigation has been carried out for zinc-nickel (Zn-Ni) electro-deposition using the constant applied current technique. Weight difference approach method was used to determine the cathode current efficiency and deposit thickness. Also, the influence effect of current density on the deposition process, solderability, and porosity of the plating layer in microelectronic applications were examined. The bath temperature effect on nickel composition and the form of the contract was studied using Scanning Electron Microscope (SEM). Moreover, elemental nature of the deposition was analyzed by Energy Dispersive X-Ray (EDX).

It has been found that the best bath temperature was 40°C, specifically at a concentration of 73 g/L of NiCl₂.6H₂O, has a milestone influence on the nickel composition and structure of the deposits. The potential is a major factor influencing the deposition coating alloy which is adjusted by the operations of the cathodic polarization; rather than the standard potential of the two metals as determined by the e.m.f. series. The anomalous deposition was obtained at a current density lower than 0.8 A/dm², while normal deposition occurred at current densities less than 1.2 A/dm².

Corrosion behavior was exhibited by the bath and for performance was carried out, and it shows that the best corrosion performance was for nickel composition of 10-12.6 wt%.

Keywords: Zinc, Nickel Alloy, Electro-co deposition, Cathodic Current density, structure.

التحقق التجريبي لترسيب سبيكة (الزنك-نيكل)

اخلاص عبدالرحمن سلمان

مدرس مساعد

كلية الهندسة-جامعة النهرين

الخلاصة

التحقق التجريبي للظروف التشغيلية لترسيب زنك نيكل باستخدام تقنية التيار الثابت المسلط . وقياس الوزن المفقود قد استخدم للحصول على كفاءة التيار الكاثودي وسمك الترسيب كذلك كثافة التيار ودرجات الحرارة لحوض الطلاء المؤثر على محتوى النيكل وتركيب السطح الذي يقود الى تحسين الخواص الكهربائية الجيدة من ناحية القابلية على اللحام وتقليل المسامية في طبقة الطلاء مما يسهل التطبيقات الألكترونية الدقيقة. وتم استخدام المسح المجهر الإلكتروني لمعرفة التركيب المجهرى للسطح وتقنية تشتت الطاقة الأشعة السينية (EDX) من اجل تحليل العناصر المكونة للطلاء. حيث وجد ان افضل درجات حرارة لحوض الترسيب الكهربائي هي 40 درجة مئوية المكون من 73 غرام من كلوريد النيكل المائي يؤثر على محتوى النيكل المترسب بينما كان جهد الترسيب من اهم العوامل المؤثرة الرئيسية في طلاء السبيكة الذي يحدد من قبل الاستقطاب الكاثودي بدلا من ان يحدد من قبل سلسلة e.m.f حيث ان الترسيب الشاذ حدث عند 0,8 امبير/دسم² والترسيب الطبيعي يحدث عند كثافة تيار اقل من 1.2 امبير/دسم² وتحقيق افضل مقاومة للتآكل عند محتوى نيكل يتراوح بين 10-12.6 % نسبة وزنية.

الكلمات الرئيسية : سبيكة الزنك، الترسيب الكهربائي، تركيب السبائك.



1. INTRODUCTION

The desired surface properties could be achieved by using co-deposition films onto surfaces much better than using single metal films. On the other hand, the co-deposition process could control several variables such as the uniformity of composition, thickness, and microstructure of the metal, **Mathias and Chapman, 1990**. It is perfectly identified that zinc alloys, for instance, Zn, Ni, Zn-Co, Zn-Fe can be responsible for fortification steel against corrosion **Tsybulskaya, et al., 2008**. In addition, as the weight of Ni content between 10 to 15% in Zn-Ni alloy, the maximum protective ability could be achieved, **Lodhi, et al., 2009**. These alloys are also considered less polluting when compared to cadmium, **Conde, et al., 2011**. The co-deposition of zinc, nickel alloy could be obtained by using different composition and operating conditions of plating baths such as sulfate-sulphamate, sulfate-chloride, pyrophosphate, cyanide chloride, sulfate and ammoniacal, **Xu, et al., 2005**.

Copper which is used as base material for electrical contacts such as printed circuits and communications equipment. But copper is material, which is exposed to decomposition. The electrical conductivity of convene resource can be mostly reduced by decomposition and in turn to pass up corrosion, preventative surfaces be used. This can be a performance for decomposition preventative of electrically conductive surfaces, to make soldering easier and the porosity is able to mostly reduce by optimization of a plating method. There are mainly two groups of materials; the primary group contains good metals such as palladium, gold, and silver. The following group consists of decomposition resistant alleged passive metals for instant tin and nickel. These metals are mainly ignoble and they take their decomposition resistance from the existence of a thin oxide film on the surface, describe the passive film, which acts as a defending impediment between the metal and its surrounding with a thickness of nanometers. Therefore one of the aims of the optimization of zinc-nickel (cheap plating) is the minimization of the size of pores, high electrical conductivity, and easier soldering. This is also one of the objectives of this investigation. This study, therefore, seeks to optimize the deposition parameters essential to obtain the range of nickel percentage in the coatings for best corrosion prevention, cathodic current efficiency, current density and temperatures for enhanced electrical properties.

1.2 Mechanism of Zn-Ni Co-deposition :

Most studies on the co-deposition of Zn-Ni have been made with acid baths which are not appropriate for steels with tensile strength more than 1510 MPa because of their high vulnerability to hydrogen embrittlement, **Jiang, et al., 2005**. Moreover, the bad environmental effect of ammonia chloride which exists in many commercial baths causes a lot of problems, **Davis, 2000**. The term anomalous co-deposition (ACD) is created to describe an electrochemical deposition process in which the less noble metal with most plating conditions is deposited preferentially.



This behavior is typically observed in co-deposition of iron-group metals, with Zn or Cd. In the deposition of Ni-Zn alloys, for instance, adding such ion some models have been proposed to explain the ACD of Zn-M alloys. Other performances have been described for electroplating of Ni-W or Re-M alloys. Generally, the electrodeposition of Zn-Ni is a co-deposition of the



anomalous type since the less noble metal Zn deposits preferentially to Ni. However, the co-deposition of Zn and Ni is not always typical at low current densities; but it can get typical deposition where Ni deposits favorably to Zn, **Gezerman, and Corbacioglu, 2010**. Therefore, in order to start anomalous co-deposition there should be a transitional current density that has to be reached. There is still no universally accepted theory in spite of several efforts that have been made to clarify the typical co-deposition of alloys, but, the theory of typical co-deposition has relied to pH increase at the cathode surface as it makes zinc hydroxide precipitation, which prevents Ni discharge. This theory does not clarify the strong inhibition of Ni reduction observed in the typical deposition region, the high current efficiency during typical deposition and the increase in the Ni content of the alloy with increasing pH. Lately, Zn-Ni co-deposition was studied as polarization curves and impedance spectroscopy measurements together in chloride and in sulfate baths. The reaction models proposed are substantially comparable and involve many adsorbed intermediates. Especially, at high cathodic polarizations (typical co-depositon) Zinc favored discharge is attributed to the intermediate, catalyst for the deposition of Zn rich deposits. At low cathodic polarization (typical co-deposition) the deposition of nickel-rich alloys was related to a mixed intermediate, which catalyzes the reduction of Ni^{2+} ions. The morphology of the coatings, as it is in their mechanical characteristics. It is necessary to note that small changes in operating conditions do not lead to substantial parameters, for instance, current density, pH, organic additives, buffer capacity, and changes in Ni content from the optimum, **Chao, et al., 2007**. Since the range of Ni content in the alloy deposit for maximum corrosion resistance is quite narrow. The need to optimize these variables to obtain the required optimum deposit composition is crucial.

2. EXPERIMENTAL

2.1 Electrolyte Preparation

The electrolyte solution was prepared by dissolving different chemical materials in annular grade in deionized water as shown in **Table 1, Zhi-Feng, 2012**.

The solution acidity (PH) was adjusted between 5.3-6.3 by adding a suitable amount of H_3BO_3 . Moreover, the temperature of the bath was kept between 18-29°C.

2.2 Electrochemical Measurements

The present work illustrates the laboratory design of electroplating system as shown in **Fig.1** where polarization curves were recorded at a sweep rate of 50 mV s^{-1} .

The electrical circuit was connected to the reference electrode saturated calomel electrode (SCE) after checking all the electrical connections. At each setting of the resistance, potential and cathodic current was recorded by a voltmeter and the ammeter to measure the cathodic portion of polarization curve. And measuring the effect of temperature on the surface morphology on plating layer at 30°C, 35°C and 40°C were considered using Scanning Electron Microscope (SEM), type Inspect S50 Netherland origin, Energy Dispersive X-Ray (EDX), porosity and Solderability tests.



2.3 Working Cathode

It was a copper cathode with purity of (98%). The cathode with area dimensions (1cm²) was prepared before each experiment by treating the surface with alkali solution (sodium carbonate 10g/l, 5g/l ethylene glycol and 5g/l sodium hydroxide) for 5 min, and then rinse with deionized water for several times to be sure that the surface is free from any trace of alkali solution. After that dipping in HCl (3% volume concentration) is used. The cathode was ready to be used in bath plating. The anode was a plate of pure metal (nickel and zinc 99.8%) the dimension of each anode 5*2*2 cm.

2.4 Determination of Cathode Current Efficiency

Energy Dispersive X-Ray (EDX) (Department of Physics, College of Science, Al-Nahrain University) was used to determine the chemical composition of (Zn-Ni) deposition layer. Specimens are weighed before and after plating where this is required for calculating the cathode current efficiency, **Lowenheim, 1974**. as follow:

$$CCE = \frac{\Delta W \left(\frac{wt\%Ni}{M_{Ni}} + \frac{wt\%Zn}{M_{Zn}} \right) * 2F}{j_{At}} 100\% \quad (3)$$

2.5 Corrosion rate by Weight Loss Technique

Weight loss of Zn-Ni surfaces to evaluate the corrosion rate of the specimen after immersion in a 3.5 % weight sodium chloride (sea water) at 25°C in static medium for six days period, and the corrosion in the second case is measured with shaking rate of 50 rpm included, In this case, the tested specimen and the corrosive medium are in dynamic conditions for five hours experimental ran, where, weight loss was measured in each hour. Corrosion rate was calculated using the equation below after measuring the weight before and after plating. **Lowenheim, 1974**.

$$C.R = \frac{\Delta w}{t * A} \quad (4)$$

2.6 Porosity Test:

Porosity test is evaluated by saturated technique, which is done by immersion the specimen in a measuring inside mercury porosimeter (Rusk instrument company) with different thickness by SEM, type Inspect S50 Netherland origin, then the weight of specimen was measured before and after immersion. This test was achieved in Petroleum Engineering Department at the University of Baghdad.

2.7 Solderability Test:

Solderability test was performed by using oven reflow process under operating conditions ranging from 240 -260°C and 1-2 minutes and then immersion in flux bath after drying passing through oven, where the sample is exposed to hot air from both sides. This test is accomplished in Scientific Research and Development Center at the Ministry of Industry and Minerals/ Iraq.

3. RESULT AND DISCUSSION

3.1 Effect of Current Density on Electro Co-deposition

It can be seen from **Fig.2** and **3**, that nickel deposit is decreased compared with zinc deposit when cathodic current density is increased. A declining in nickel deposition and rising in zinc deposition with increasing current density this may be due to the more rapidly mobility of zinc deposition at larger electrode polarizations. The effect signs that at decrease assess of current density near the transition from anomalous to normal co-deposition, anomalous state of co-deposition has been generally explained using the hydroxide inhibition type of regions of co-deposition. So, it is not a generalized model, while at lower current densities, the normal deposition will take place, where the more noble metal deposits preferentially. When the current density is increased, a transition will occur from normal to up normal deposition, with noble metal deposit amount be lower than the concentration of the metal in the bath. These phenomena consequences of the formation of a critical concentration of zinc hydroxide at the cathode surface which apparently hinders the discharge of Ni ions due to adsorption of zinc hydroxide formed as a result of alkalization near the cathode surface during intense hydrogen evolution.

3.2 Effect of Current Efficiency:

It is clear from **Fig.4** that increasing cathodic current density will decrease cathodic current efficiency. This may be attributed to the fact that co-deposition (alloy deposition) performance is affected by the applied current density where at low values of current density the normal deposition type will take place with poor current efficiency. While at higher values of deposition of less noble Zn will take place rather than the co-deposition so the alloy composition hardly tends to change. Beyond that region where Ni percentages of the alloy increase with an increase in current density even though, relatively high current efficiency for co-deposition is still preserved.

3.3 Effect of Electrolyte Temperatures:

Fig 5, 6, and 7 show the influence of bath temperature (30, 35, 40 °C) on the cathodic polarization curves which results in a limiting current density between 10-20 mA/cm². The data show that the reduction potentials of nickel become nobler with an increase in electrolyte temperature. Moreover, because of elevating the electrolyte temperature, the cathodic polarization will decrease. It is well known that by increasing electrolyte temperature the concentration of the two ions (zinc and nickel) in the cathode diffusion layer will increase because the rate of diffusion increases with temperature. Moreover, increasing the electrolyte temperature decreases the activation polarization of the zinc ions; such effect returned in a decrease in cathodic polarization. In order to explain that effect, the SEM and EDX tests were considered to analyze the deposit. In general, any change in electrolyte temperature will influence the deposit structure. It was noticed that the electrolyte temperature effect on the microstructure of co-deposition smoothens of the surface and finally the grain size, which may affect on corrosion efficiency of that deposit.

3.4 Structure of (Ni-Zn) Electrodeposits:

Investigation of electrodeposited layers by scanning electron microscopy exposed differences in surface morphology of Ni-Zn obtained at different conditions such as current density and temperature. The influence of current density (8 mA/cm², 12 mA/cm² and 14 mA/cm²) on the SEM surface morphology of (Ni-Zn) layer is described in **Fig. 8 a, b, and c** respectively. When increasing the current density, the crystallite size of nickel zinc layer becomes larger. Identical and uniform coatings is obtained with current density 12 mA/cm². While other deposits show less uniformity and having a branched form resembling a tree.

Fig. 8 d, e, and f and **Fig.9 a, b, and c** show the SEM surface morphologies and compositional analysis by EDX at three temperatures (30, 35, 40° C) at current density 12 mA/cm² during the co-deposition time of 18 min. It was noted that when the temperature raised five degrees (35-40 °C) the deposited shape will change from crystal hierarchical and irregular into a regular shape and homogeneous surface gives good mechanical and electrical specifications for reduced porosity with good solderability in addition to increased corrosion resistance.

3.5 Corrosion Resistance:

The corrosion rate was determined by using the classical weight loss technique for the following cases:

Case 1. The corrosive media (saline water) is static for five days period.

Case 2. When introducing mechanical vibration in two ways, the first is shaking the specimen with corrosive media together, the second is when the samples and corrosive media are fixed, for each way the total test duration was five hours. **Fig 10** shows the C.R with time for the first case. From **Fig. 10, 11** it is noticed that the corrosion rate in the static and vibrating media reached the highest value in the first hours and began to decrease after five hours daily for a week. This may be due to the oxide layer resulting from interaction with zinc-nickel layer on the surface of the existing substrate lower solubility of metal and reaction with oxygen and thereby stop the reaction.

3.6 Porosity with Different Thickness:

Specimens were examined with different thickness between 1-5µm and the percentage of the porosity ranging from 45-53%, but the percentage of samples of thickness between 10-18 µm 10-5% as shown in **Fig.12**

It can be noticed that porosity for the plating film will decrease by increasing thickness. The porosity test showed that the best plating thickness (less porosity) was 18 µm.

3.7 Solderability for Plating:

Specimens which were exposed to solderability showed that the high nickel content in plating layer improves the good solderability about (229-233° C) while low nickel content leads to cracking in surfaces and bad solderability. This may be due to the natural crystal structure of zinc metal.



4. CONCLUSIONS

The present work has been mainly intended to find a relationship between current densities with co-deposition (nickel and zinc), also to study effect of current on cathodic current efficiency and bath temperature and from effect on structure and nickel weight percentage which is enhancement corrosion resistance, porosity and solderability is the effect for improvement the microelectronic application as follows:

1. Cathodic current efficiency decreases with increasing current density.
2. Nickel weight percentage deposition decreases with increasing current density.
3. Optimum bath temperature 40°C for electrolyte solution as: 171 g/l NH₄Cl , pH=5.3-6.3, 73.9 g/l NiCl₂.6H₂O, 60.7 g/l ZnCl₂, 20 g/l H₃BO₃, temperature of bath 40°C, Time 18 min.
4. Surfaces structure has been analyzed by SEM were successfully electroplated onto copper substrate was found smooth and adherent.
5. In addition to obtaining a high resistance to corrosion by coating the copper instead of steel must note that choice of copper for modification of the mechanical and electrical properties.

REFERENCES

- Bodaghi, A., and Hosseini, J., 2012, *Corrosion Behavior of Electrodeposited Cobalt-Tungsten Alloy Coatings in NaCl Aqueous Solution*, *Int. J. Electrochem. Sci.* vol 7, PP 2584 – 2595.
- Boonyongmaneerat, Y., Saenapitak, S., and Saengkiattiyut, K., 2009, *Alloys Compd.* PP.487 479
- Binkauskene, E., 2002, *Influence of Operation Parameters on Metal Deposition in Bright Nickel-plating Process*, *Rus. J. Appl. Chem.* No. 75.
- Chao-qun ,L., Xin-hai, L., and Zhi-xin , 2007, *Transition Nonferrous Metals Soc. China* vol.17, PP1300.
- Conde , A., Arenas, M.A., and de Damborenea, J.J., 2011, *Experimental methods designed for measuring corrosion in highly resistive and inhomogeneous media*, *Corros. Sci.*vol. 53, No.4,PP1450-1550.
- Davis, R.D.,2000, *Nickel, Cobalt and their Alloys*. ASM International Handbook Committe. U.S.A., PP.106-107.
- Fratesi, G. R, Giuliani, G., and Tomachuk, C.R., 1997, *Zinc-cobalt alloy electrode-position from chloride baths*, *J. Appl. Electrochem.* , vol.27 PP.1088–1094.
- Goodwin, F. E., in Proc. 1998, 4th Int. Conf. *on Zinc and Zinc Alloy Coated Steel Sheet (Galvatech, 98)*, Chiba, Japan, The Iron and Steel Institute of Japan, PP. 31–39.



- Gaevskaya, L. S., and Purovskaya, T.V., 2008, *Structural Characterization and Mechanical Properties of As-plated and Heat Treated Electroless Ni-B-P Alloy Coatings*, *Surf. Coat. Technol.*, Vol. 203, PP 234
- Gezerman, A.O.,and Corbacioglu, B.D., 2010, *Int. J. Chem.* 2 124.
- HovestadL, A.,and Janssen ,J. J. 1995, *Electrochemical codeposition of inert particles in a metallic matrix*, *journal of Applied Electrochemical*, , Vol. 25, No.25, pp 519–527
- Jiang, Y.F., Liu, L.F. , Zhai, C.Q., and Ding, W.J., 2005, *Thin Solid Films*, PP 484 232
- Lowenheim, F. A., 1974, *Modern Electroplating*, 3rd ed., Wiley, New York.
- Landolt, D., 2007, *Corrosion and Surface Chemistry of Metals*; pp. 227–274
- Mathias, M.F. and Chapman, T.W., 1990, *Zinc-Nickel Alloy Electrodeposition Kinetics Model from Thickness and Composition Measurements on the Rotating Disk Electrode*, *Journal of Electrochemical Society.*, Vol.137, No.1.PP.102-110.
- Parsons, R., 1959, *Handbook of Electrochemical Constants*, Butterworths Scientific, London.
- Xu, Q., Telukdarie, A., Lou, H.H., and Huang, Y., 2005, *Ind. Eng. Chem. Res.* 44 2156. 10.1021/ie0495067
- Zhi-feng L., Xiang-bo L., and Li-kun Xu, 2012, *Electrodeposition and Corrosion Behavior of Zinc-Nickel Films Obtained From Acid Solutions: Effects of TEOS as Additive*, *Int. J. Electrochem. Sci.*, vol.7 ,PP.12507- 12517

NOMENCLATURE :

- A: cathode surface area (cm^2)
CCE: cathode current efficiency, (%)
C.R: corrosion rate ($\text{g/m}^2\text{day}$)
F: Faraday constant (96500 C/mol)
j : current density (A/dm^2)
 M_{Ni} : atomic weight of nickel (g/mol)
t: plating time(second or day)
 ΔW : weight difference after plating, (g)
wt%Ni: weight percentages of nickel
wt%Zn: weight percentages of zinc

Table 1. The composition of Zinc-Nickel plating bath.

Component	g/l
NH ₄ Cl	171
NiCl ₂ .6H ₂ O	73.9
ZnCl ₂	60.7
H ₃ BO ₃	20

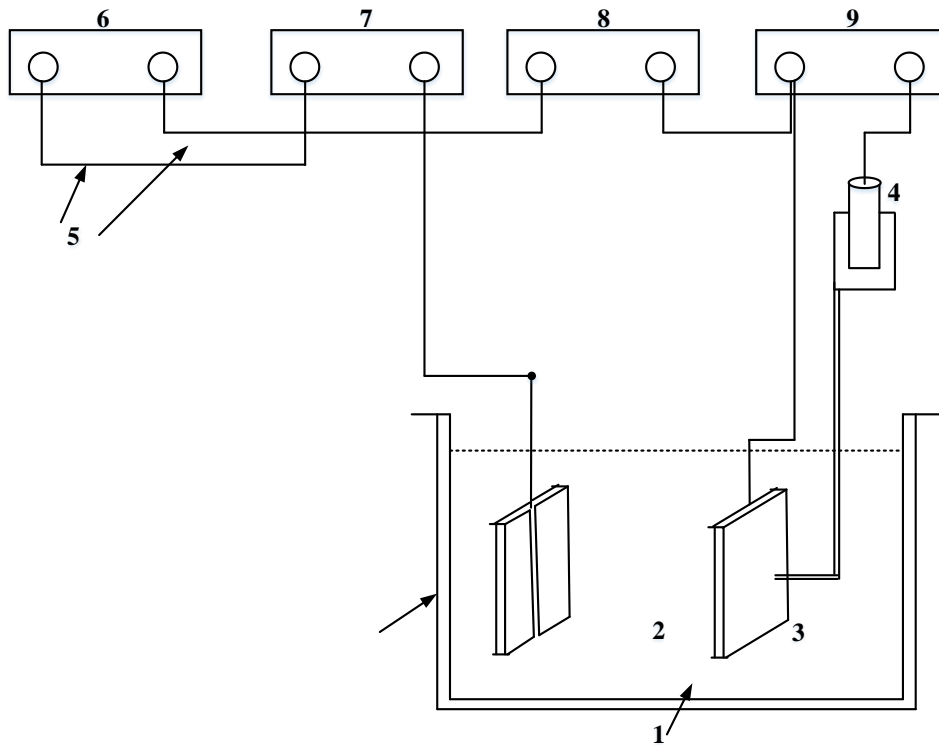
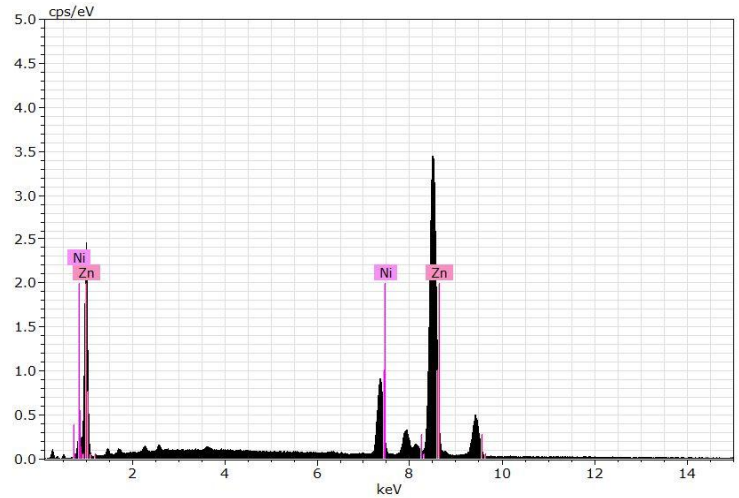


Figure 1. A simple sketch illustrating the details of the laboratory.

Table 2. The item numbers with details as illustrated in Fig. 1.

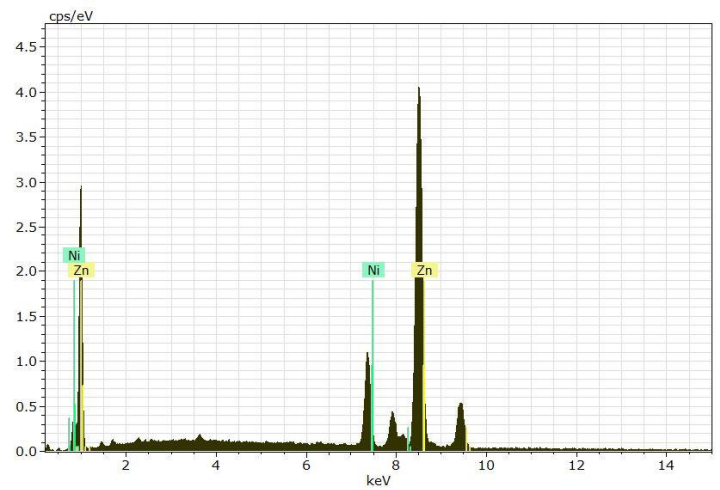
Item No.	Name
1	Plating Solution
2	Zinc -Nickel anode (5x2x2)cm
3	Cathode (1)cm ²
4	Saturated calomel electrode (SCE)
5	Connecting wires
6	D. C. power supply
7	Multi-range Ammeter
8	Resistance Box
9	Multi-range Voltmeter

Bruker Nano GmbH, Germany		5/15/2016		
Quantax				
Results	Objects 15786			
Date:	5/15/2016			
Element	AN	series	[wt.%]	[norm. wt.%]
Zinc	30	K-series	62.0262	33.9
Nickel	28	K-series	120.9419	66.0999
		Sum:	182.9681	100



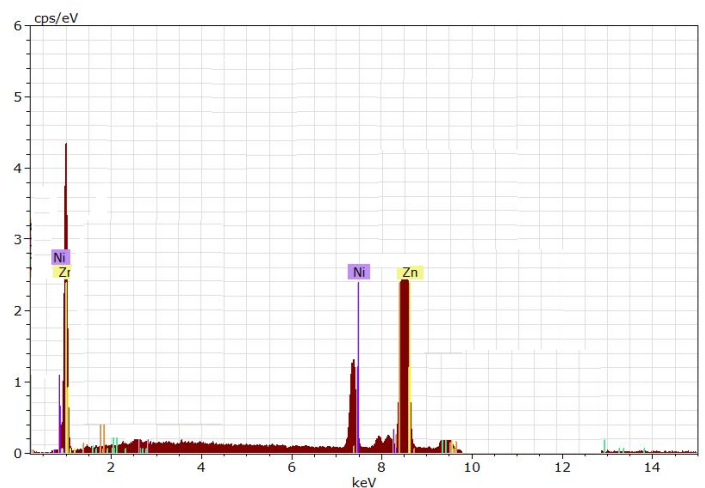
(a)

Bruker Nano GmbH, Germany		5/15/2016		
Quantax				
Results	Objects 15786			
Date:	5/15/2016			
Element	AN	series	[wt.%]	[norm. wt.%]
Zinc	30	K-series	84.61598	44.5601
Nickel	28	K-series	105.27582	55.4398
		Sum:	189.8918	100



(b)

Bruker Nano GmbH, Germany		5/15/2016		
Quantax				
Results	Objects 15786			
Date:	5/15/2016			
Element	AN	series	[wt.%]	[norm. wt.%]
Zinc	30	K-series	79.7204	46.3440
Nickel	28	K-series	92.2947	53.6538
		Sum:	172.0187	100



(c)

Figure 2. EDX of Zn-Ni for different current density (a) 8 mA/cm² (b) 12 mA/cm² (c) 14 8 mA/cm² ° for 171 g/l NH₄Cl , pH=5.3-6.3, (2) 73.9 g/l NiCl₂.6H₂O, 60.7 g/l ZnCl₂, 20 g/l H₃BO₃.

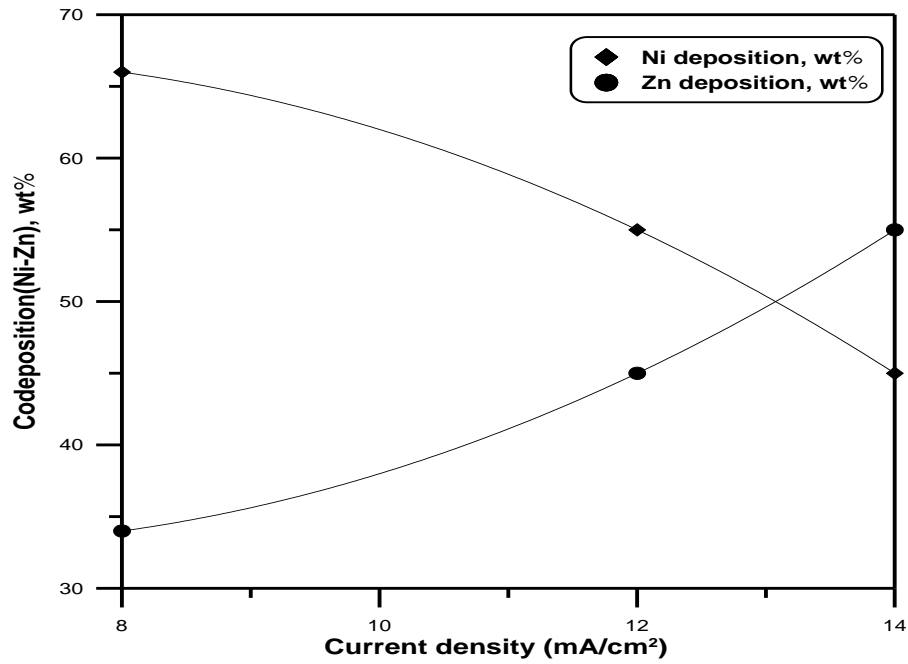


Figure 3. Effect of current density on nickel deposition from Chloride bath containing 171 g/l NH₄Cl , pH=5.3-6.3, 73.9 g/l NiCl₂.6H₂O, 60.7 g/l ZnCl₂, 20 g/l H₃BO₃,tempeture of bath 18-29°C.

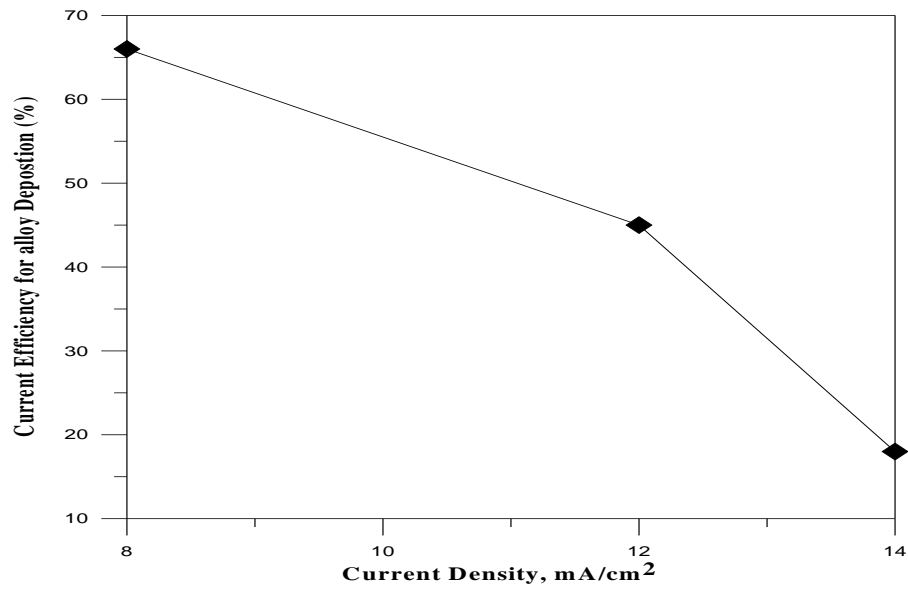


Figure 4. Cathodic efficiency vs Cathodic Current density.

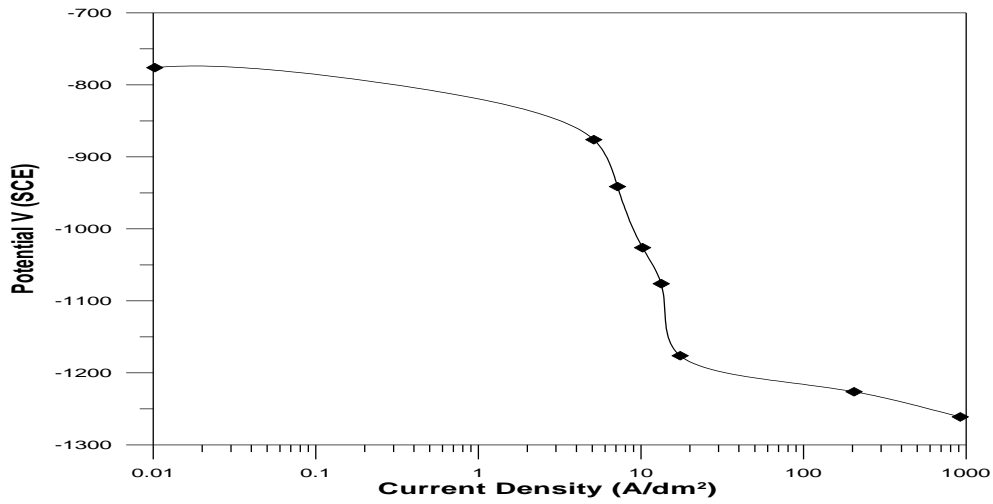


Figure 5. Polarization Curve of Ni-Zn during the electro deposition at (8.5mA/cm²) and 30°C.

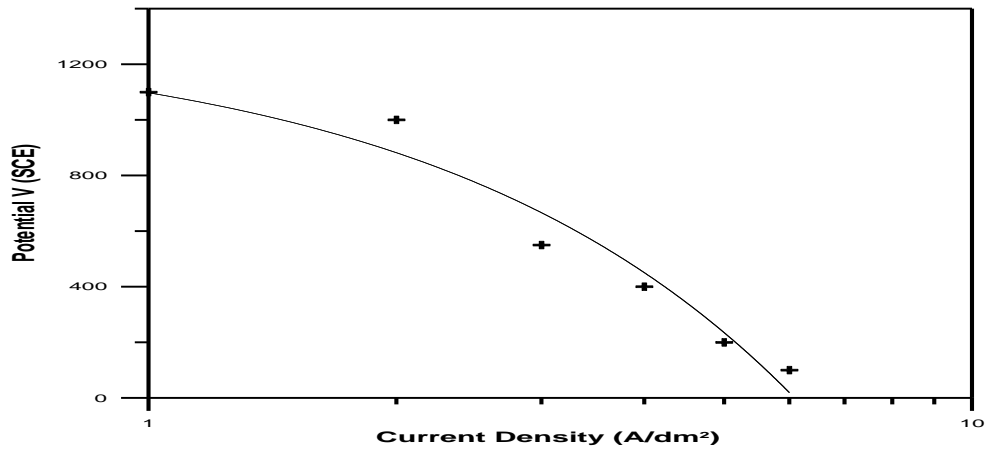


Figure 6. Polarization Curve of Ni-Zn during the electro deposition at (12 mA/cm²) and 35°C.

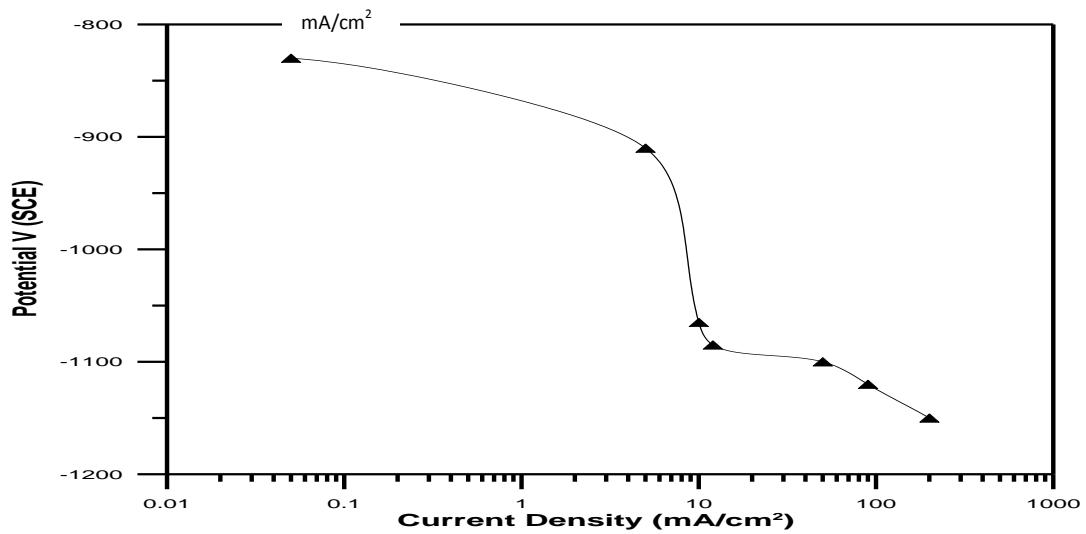
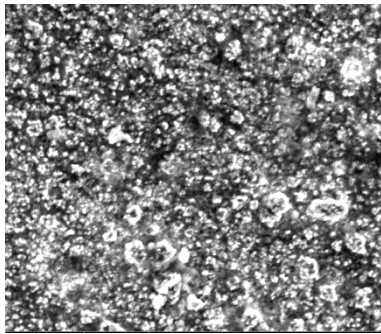
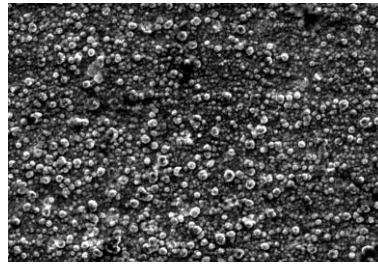


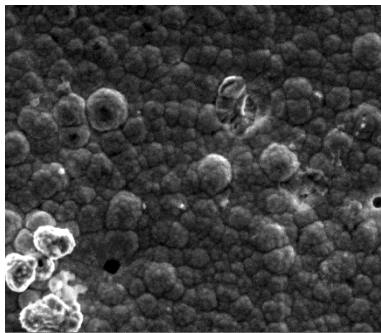
Figure 7. Polarization Curve of Ni-Zn during the electro deposition at (12 mA/m²) and 40°C.



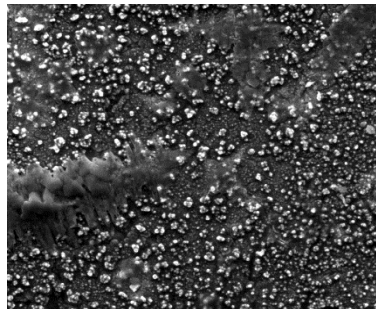
(a)



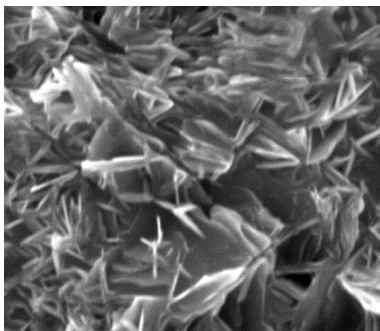
(b)



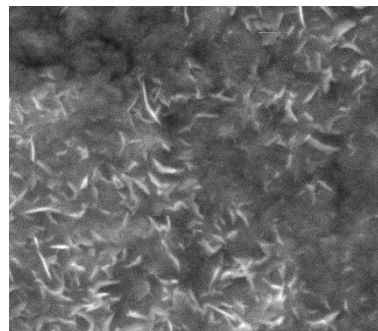
(c)



(d)



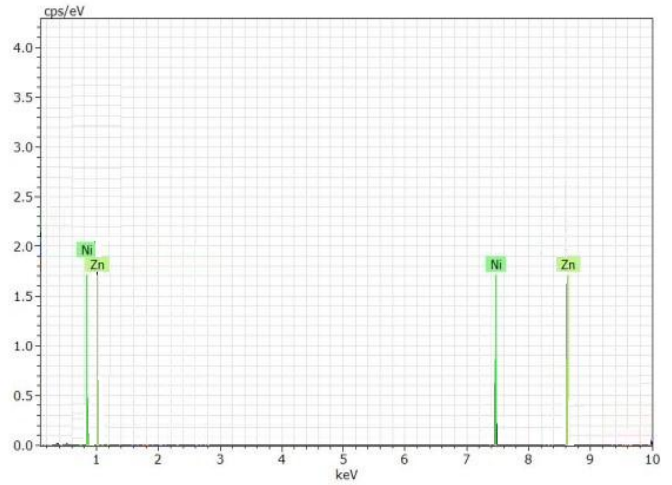
(e)



(f)

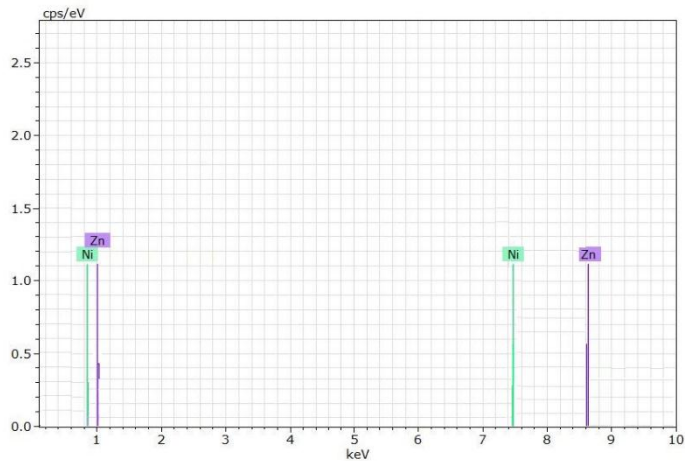
Figure 8. SEM of Zn-Ni for different conditions of current density and temperatures (a) $8\text{mA}/\text{cm}^2$ (b) $12\text{mA}/\text{cm}^2$ (c) $14\text{ mA}/\text{cm}^2$ (d) 30 C° (e) 35 C° (f) 40 C° for $171\text{ g}/\text{l NH}_4\text{Cl}$, $\text{pH}=5.3-6.3$, (2) $73.9\text{ g}/\text{l NiCl}_2\cdot 6\text{H}_2\text{O}$, $60.7\text{ g}/\text{l ZnCl}_2$, $20\text{ g}/\text{l H}_3\text{BO}_3$, temperature of bath 30 C° .

Bruker Nano GmbH, Germany		5/15/2016		
Quantax				
Results	Objects 15786			
Date:	5/15/2016			
Element	AN	series	[wt.%]	[norm. wt.%]
Zinc	30	K-series	51.96774	34.66431
Nickel	28	K-series	97.94938	65.33569
		Sum:	149.9171	100



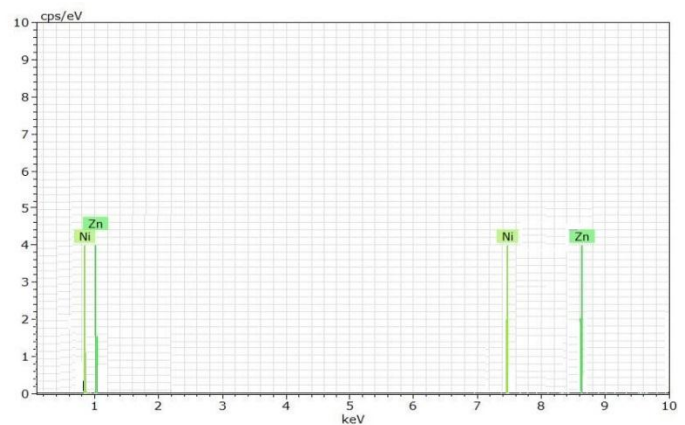
(a)

Bruker Nano GmbH, Germany		5/15/2016		
Quantax				
Results	Objects 15786			
Date:	5/15/2016			
Element	AN	series	[wt.%]	[norm. wt.%]
Nickel	28	K-series	82.45	52.16291
Zinc	30	K-series	75.6125	47.83709
		Sum	158.0625	100



(b)

Bruker Nano GmbH, Germany		5/15/2016		
Quantax				
Results	Objects 15786			
Date:	5/15/2016			
Element	AN	series	[wt.%]	[norm. wt.%]
Nickel	28	K-series	89.76022	67.27701
Zinc	30	K-series	43.65863	32.72299
		Sum:	133.4189	100



(c)

Figure 9. EDX of Zn-Ni for different temperatures of bath (a) 30 C° (b) 35 C° (c) 40 C° for 171 g/l NH₄Cl , pH=5.3-6.3, (2) 73.9 g/l NiCl₂.6H₂O, 60.7 g/l ZnCl₂, 20 g/l H₃BO₃, current density 12 mA/cm².

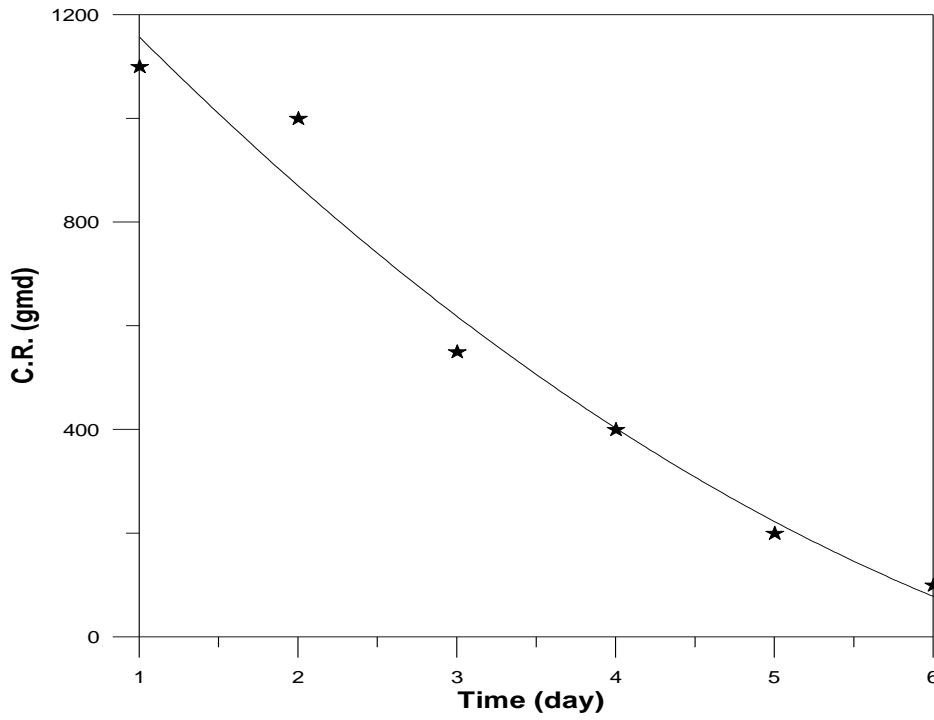


Figure 10. The relationship between time and the rate of corrosion in static corrosive medium.

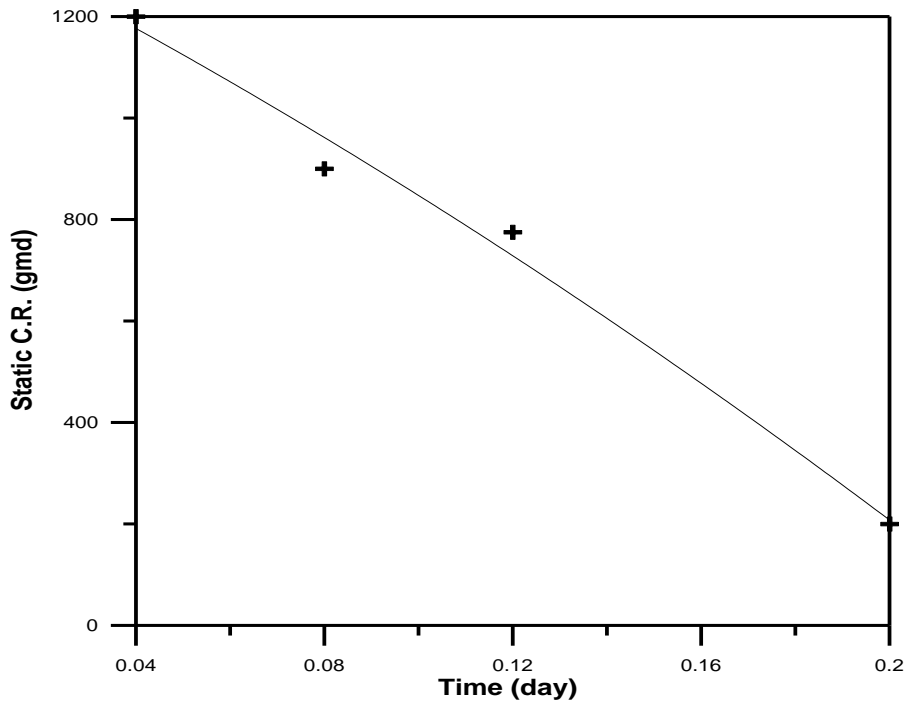


Figure 11. The relationship between time and the rate of corrosion happening in the media corrosive vibration.

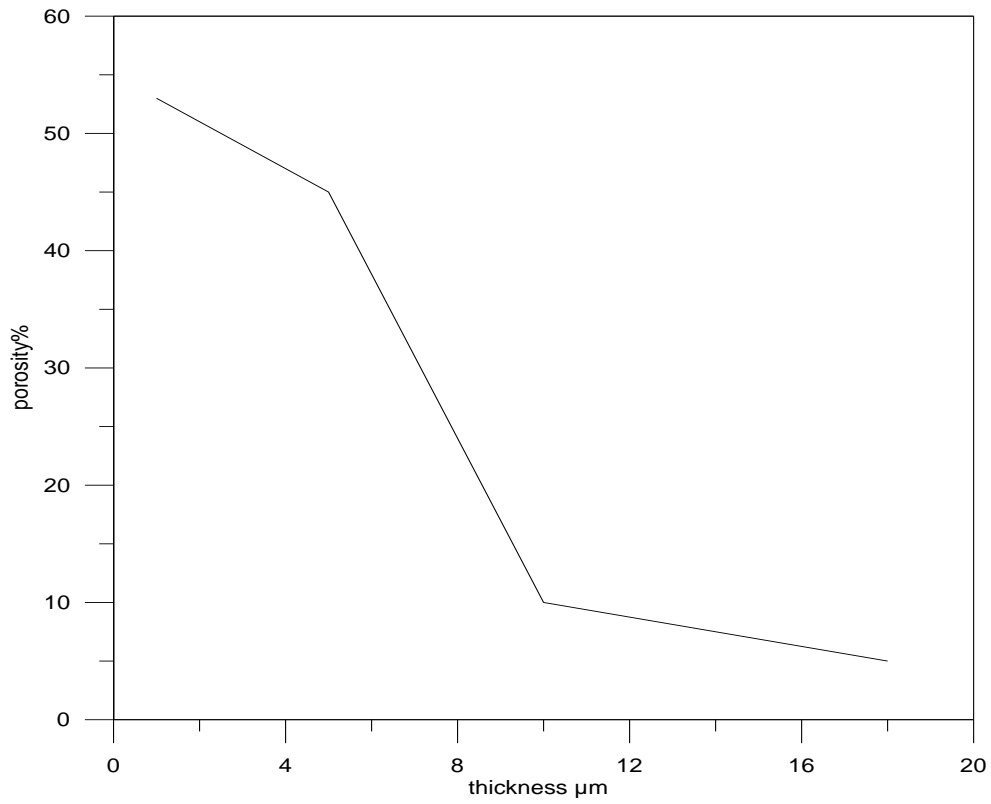


Figure 12. The porosity of zinc- nickel plating with different thickness.